Effect of shoulder model complexity in upper-body kinematics analysis of the golf swing

Bourgain M[1], Hybois S[1], Thoreux P[2], Rouillon O[3], Rouch P[1], Sauret C[1]

[1] Institut de Biomécanique Humaine Georges Charpak, Arts et Métiers ParisTech, Paris, France

[2] Hôpital Avicenne, université Paris 13, Sorbonne Paris-Cité, AP-HP, 93017 Bobigny, France

[3] Fédération Française de Golf, 68 rue Anatole France, 92309 Levallois Perret, France

Abstract

The golf swing is a complex full body movement during which the spine and shoulders are highly involved. In order to determine shoulder kinematics during this movement, multibody kinematics optimization (MKO) can be recommended to limit the effect of the soft tissue artifact and to avoid joint dislocations or bone penetration in reconstructed kinematics. Classically, in golf biomechanics research, the shoulder is represented by a 3 degrees-of-freedom model representing the glenohumeral joint. More complex and physiological models are already provided in the scientific literature. Particularly, the model used in this study was a full body model and also described motions of clavicles and scapulae. This study aimed at quantifying the effect of utilizing a more complex and physiological shoulder model when studying the golf swing. Results obtained on 20 golfers showed that a more complex and physiologically-accurate model can more efficiently track experimental markers, which resulted in differences in joint kinematics. Hence, the model with 3 degrees-of-freedom between the humerus and the thorax may be inadequate when combined with MKO and a more physiological model would be beneficial. Finally, results would also be improved through a subject-specific approach for the determination of the segment lengths.
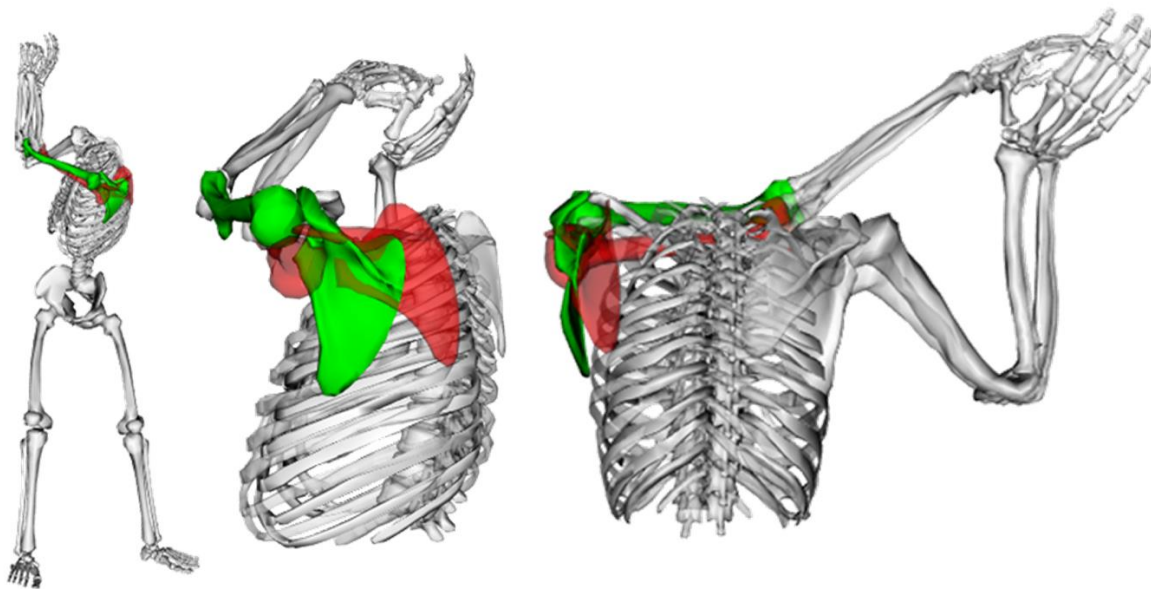
Figure 3: Visualization from front and lateral views of the left scapula and humerus of a subject obtained using MP (green) and MS (red). Reader should refer to the online version of the paper for color visualization.

Introduction

The golf swing is a complex movement involving the whole body. If low back pain is the most common injury among golf players (Cole and Grimshaw, 2014; Gluck et al., 2008; McHardy and Pollard, 2005) and represents up to 34% of all injuries linked to the golf swing, shoulder injuries represent up to 18% (McHardy et al., 2006; Perron et al., 2016). From a performance point of view, one of the key-parameters is the X-factor (Joyce et al., 2010; Kwon et al., 2013; Myers et al., 2008) that represents the global dissociation angle between shoulders and pelvic girdle. The relative movement between shoulders and thorax is often assumed to be negligible (Healy et al., 2011). However, in an exploratory study based on medical images, the role of the whole shoulder complex was highlighted in a static position, which was close to top of backswing position. In this study, the axial rotation between shoulders (line between the two acromions) and thorax were found to contribute to more than 40% of the one between shoulder and pelvis (Bourgain et al., 2016). Since the relative contribution of the spine and the shoulders vary between subjects, it could result in excessive participation of shoulder joints and/or spine joints, and could be decisive in the occurrence of low back pain and shoulder injuries. Hence, a biomechanical analysis of the golf swing can be beneficial for the understanding of the etiology of these injuries and the development of prevention procedures.

Quantifying the kinematics during a golf swing is necessary for any biomechanical analysis. However, spine and shoulder motions are difficult to record. Generally, in golf biomechanics, the shoulder is reduced to the glenohumeral joint (GHJ) (Egret et al., 2004, 2003; Nesbit, 2005) which kinematics were obtained from the orientation of the humerus with respect to the thorax. However, the shoulder is a more complex structure that involves several joints working in a closed-loop kinematic chain, *i.e.* the sternoclavicular joint (SCJ) between the sternum and the clavicle; the acromioclavicular joint (ACJ) between the clavicle and the scapula; the scapulothoracic joint (STJ) between the scapula and the thorax, and the GHJ between the humerus and the scapula. In addition, motions of all these bones are difficult to record without invasive or irradiant procedures (Dal Maso et al., 2014; Matsui et al., 2006; McClure 2001) and there is a lack of knowledge about soft tissue artifact (STA) occurring in this region (Blache 2016). As multibody kinematic optimization (MKO) takes into account joint degrees of freedom (DoF) for computing joint kinematics by minimizing the distance between experimental and simulated markers attached to segments, some authors recommend to use it for limiting the effect of STA (Lu and O'Connor, 1999; Seth et al., 2016; Blache et al., 2016; Duprey et al., 2016; Naaim et al., 2015). However, the accuracy of this technique fully relies on the kinematic chain model used to represent the subject and some authors measured an increase of the error with the use of MKO technique (Anderson et al. 2010).

Many shoulder models are related in the literature (Duprey et al., 2016). Globally, two main categories can be distinguished: models only considering GHJ with the scapula fixed in the thorax frame, versus models allowing the scapula to glide over an ellipsoid representing the thorax, generally with a constraint due to the clavicle length. While the second category obviously appears more physiologic, the scaling of these models to individuals is not trivial (Prinhold and Bull, 2014; El Habachi et al., 2015; Duprey et al., 2017; Naaim et al., 2017) and may result in inaccurate kinematics. In addition, the effect of the model complexity would be either crucial or negligible depending on the studied movement. Until now, no study has quantified the influence of a complex but more physiological shoulder model for the calculation of upper-body kinematics during the golf swing.

In order to fill this lack of knowledge, the aim of this study was to quantify the effect of utilizing a more complex shoulder model for studying kinematics during the golf swing through MKO.

Material and Methods
Experiments
20 golfers were volunteers to participate in this study (Table 1). They were previously informed about the protocol and signed a written informed consent form prior to the beginning of the experiments. The protocol was approved by an independent ethics committee (2015-A01760-49, Ile de France X).

Participants were equipped with 65 reflective markers allowing a full-body analysis (Figure 1 and supplementary material), in an indoor motion analysis laboratory. Each participant performed his personal warm-up routine including swings to get used to the experimental setup, followed by a static acquisition in a reference anatomical position. Then, volunteers performed a series of 10 measured swings with their personal driver. Markers trajectories were tracked by a 12-cameras optoelectronic motion capture system (Vicon system, Oxford metrics, UK; 200 Hz). The swing performance was obtained through a golf launch monitor (TrackMan 3, Trackman, USA) and the swing exhibiting the maximal club head velocity at the impact was selected for analysis.

Data processing and multibody model
Data were processed through a MKO technique implemented in OpenSim3.3 software (Delp et al., 2007). For that purpose, a full-body model was created based on the model of Raabe (Raabe and Chaudhari, 2016) where the shoulders were modified by the STJ model of Seth (Seth et al., 2016). For the shoulder, it resulted in 2 rotational DoF for SCJ, 3 rotational DoF for ACJ (through a point constraint between the clavicle and the acromion), 3 rotational DoF for GHJ, and a contact ellipsoid for the STJ. All the DoF were unclamped to avoid the effect of joint magnitude limitation. Thus, the generic fullbody model has 25 segments with 54 generalized coordinates with 2 constrains for ellipsoid joints between scapula and thorax. Besides, DoF of the lumbar spine were coupled to take into account movements between vertebrae. The generic model was then scaled (segments and contact points) to each participant based on the static acquisition. This scaled model (MP) was then used to create a second model with a simplified kinematic chain for the shoulder (MS). It was obtained by locking both the sternoclavicular and the scapulothoracic joints in the neutral position obtained in the static acquisition. Hence, MS resulted in a shoulder model reduced to the GHJ with 3 rotational DoF and with the scapula fixed in the thorax frame. All trials were processed using both models with the same computational conditions (given in the supplementary material) using the inverse kinematics tool implemented in Opensim software.

Data analysis
For both models, distances between measured and reconstructed markers during the whole swing duration were expressed individually by the root mean square distance (RMSD). To allow analysis by segment, a weighted average distance (WAD, equation 1) was calculated with all the markers belonging to the same segment. The effect of considering a more physiological model of the shoulder was investigated by the difference between results obtained using MS minus results obtained using MP. Hence lower RMSD or WAD for the MP resulted in positive value.

$$WAD_{segment} = \frac{1}{\sum\limits_{i=1:N_{Mseg}} w_i} . \sum\limits_{i=1:N_{Mseg}} RMSD(i).w_i \qquad \text{(equation 1)}$$

With: w_i weight of the marker i (Supplementary material), N_{Mseg} the number of markers attached to the segment and RMSD(i) the RMSD of the marker i.

Then, occurrence of gimbal locks (GL) were identified visually by an experienced investigator and counted. Finally joint kinematics data with GL were removed before computing angle RMSD.

Table 1: Subjects characteristics. Golf handicap is an international parameter for skill measurement. Professional golfers don't have one.

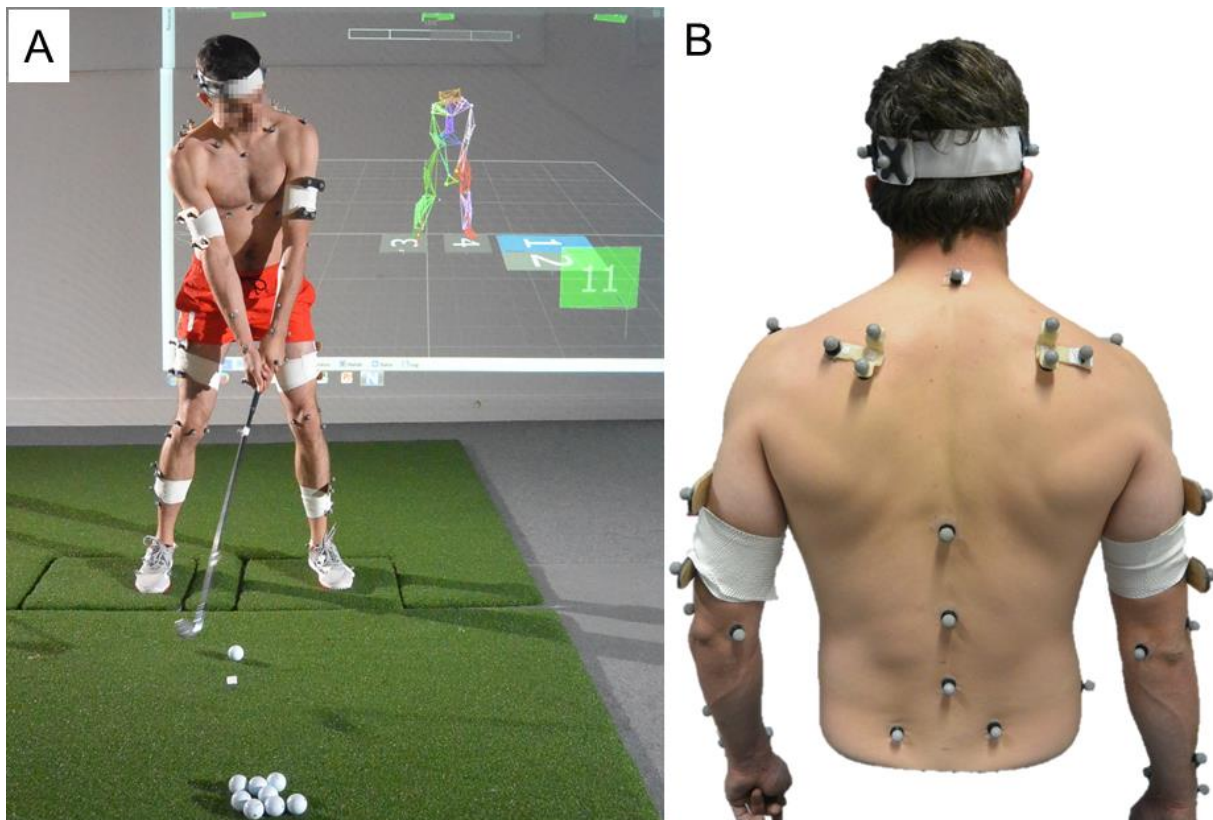|	Mean	SD	Minimum	Maximum
Golf handicap (n=13)	13.5	5.1	4.5	20
Age (years) (n=20)	44.6	17.3	22	70
Weight (kg) (n=20)	79.9	10.4	63	105
Height (m) (n=20)	1.82	0.08	1.67	1.95
Professional golfers	6			
Golf teacher	1			
Amateurs golfers	13			
Gender	Male : 19	Female : 1		
Right handed	20			
Left handed	0			

Figure 1: A : photograph of a subject equipped with the markers during an experiment (here with a 6-iron club). B : photograph of the back of a subject equipped with markers.

Table 2: Mean values, standard deviations, minimums and maximums of improvements in segment WAD (in mm). R/L for Right/Left side, respectively. Positive values mean MP simulated markers are closer to experimental markers than MS.

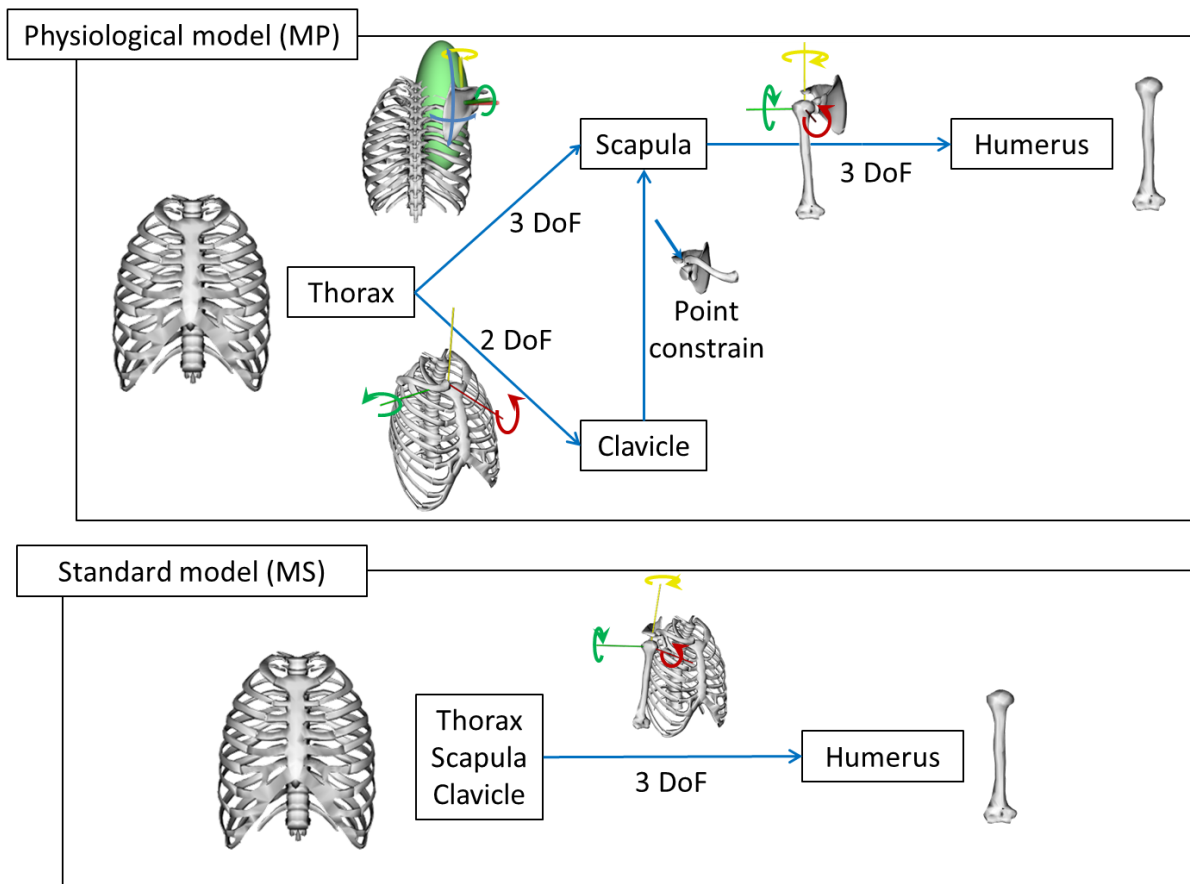|	Mean	SD	Min	Max
Thorax	0	5	-10	9
Pelvis	0	1	-2	2
Shoulder L	-3	4	-10	6
Shoulder R	8	4	0	16
Arm R	6	4	1	15
Arm L	3	6	-9	11
Forearm R	2	2	-4	5
Forearm L	6	5	0	19
Hand R	2	2	0	6
Hand L	4	4	0	15
Clavicle R	3	2	0	6
Clavible L	0	3	-8	4
Scapula L	14	9	-1	32
Scapula R	-5	8	-18	14
overall	2	5	-18	32

Figure 2: Detailed DoF modelling of the physiological model (MP) and the standard model (MS)

Results

For the 20 subjects, 6 markers exhibited a positive evolution of RMSD, of at least 10mm, from MS to MP (the three markers of the right scapula cluster, the left lateral epicondyle, the left costal technical marker and the right acromion) but 2 markers had a negative evolution between the 2 models of at least 10mm (two markers of the left scapula cluster). Lower limbs markers were slightly influenced with a variation of about 1mm.

5 subjects were noted with 11 occurrences of GL or inconsistent results, with MP. With MS, 9 subjects were noted for 33 occurrences. No kinematics results were improved with MS. Those occurrences were mainly located on left axial rotation (8 occurrences) and left pronosupination (6 occurrences).

After exclusion of subjects with GL and inconsistent results, segments WAD evolution was small for lower limbs and thorax (from -0.2mm for thorax to +0.4mm for pelvis). For shoulders and upper limbs segments, only the left scapula (-5.1mm evolution) and left full shoulder (-2.6mm evolution) had a negative WAD. All other segments have a positive WAD evolution from +0.1mm (left clavicle) to +13.7mm (right scapula).

As a consequence, joint kinematics were affected (Table 3). On average the RMSD of the lower limbs were slightly affected (1.1°, SD: 1.3°; range: 0.1° to 8.9°). The trunk DoF were more influenced with an average RMSD of 12.5° (SD: 8.2°) and ranging from 2.9 to 34.5°. Upper limbs were the more influenced with a RMSD of 10.4° (SD: 11.5°) and ranging from 0.5° to 54.2°.

Table 3: Mean values, standard deviations, minimums and maximums of angle RMSD (in degrees) between both models. R/L for Right/Left side, respectively.

DoF	Mean	SD	Min	Max
R clavicle protraction	16.0	4.9	9.1	24.7
L clavicle protraction	12.5	6.0	6.6	29.9
R clavile elevation	9.7	3.5	5.4	17.5
L clavicle elevation	11.0	5.5	4.7	21.5
R elbow flexion	4.0	1.6	2.3	7.8
L elbow flexion	4.8	2.5	1.7	9.8
R pronosupination	7.3	6.3	1.5	24.8
L pronosupination	12.0	8.7	2.5	30.9
R wrist flexion	2.9	2.2	1.4	9.7
RLwrist flexion	4.7	2.4	1.4	9.7
R wrist deviation	4.9	4.1	1.7	17.9
L wrist deviation	3.2	2.3	0.5	8.4
R shoulder	17.9	10.8	5.4	40.1

elevation				
L shoulder elevation	29.2	11.9	9.5	54.2
R shoulder flexion	13.5	7.9	3.1	32.8
L shoulder flexion	12.6	5.4	2.4	20.9
R shoulder rotation	13.2	4.7	5.8	22.3
L shoulder rotation	44.6	14.1	21.0	67.9
R scapula abduction	17.4	6.8	9.5	29.7
L scapula abduction	29.2	11.0	15.3	58.2
R scapula elevation	10.1	4.1	4.0	16.0
L scapula elevation	4.9	1.9	1.9	8.5
R scapula upward rotation	14.7	9.1	3.3	31.2
L scapula upward rotation	18.9	6.2	8.7	29.3
R scapula winging	5.3	2.4	1.8	9.6
L scapula winging	11.0	8.1	5.8	36.5
Spine flexion/extension	8.8	2.9	4.9	15.2
Spine lateral bending	7.1	3.2	2.9	13.3
Spine axial rotation	21.6	7.8	11.0	34.5
overall	12.9	11.5	0.5	67.9

Discussion

As expected, the markers which are the closest to the shoulders were the most affected by the change in shoulder kinematic chain. The differences between right and left upper limbs can be explained by the higher mobility of the left scapula (in particular at the end of the backswing), which then benefited more from the additional mobility allowed by MP. Clavicles appeared less, but positively, improved by the use of MP. This can be explained by both the reliability and the total weight (for MKO) attributed to the markers fixed on these segments. Even if the single clavicle marker was fixed on the middle part of the clavicle, which was showed to be less impacted by STA, this one remained high (Blache et al., 2017). In addition, because markers weights were attributed according to marker position reliability, several segments, such as scapulae and clavicles, were less weighted than the others (such as thorax for example). As translation and some rotations (assumed to be non-physiological) were not allowed between segments in both models, errors induced by a poor definition of shoulders may spread to more distal segments such as hands. As a result, markers of the hands were slightly but positively affected by the use of the MP.

In essence of the MKO technique, the change in RMSD between reconstructed and experimental markers resulted from a change in the generalized coordinates (i.e. joint angles). Hence, joints kinematics were altered by the change of shoulder model. In particular, as scapulae were fixed to the thorax, a difference of 68° was noted in left humeral axial rotation for one subject. This can be explained by the absence of scapula abduction in MS; and, to a smaller extent, by the locked translation of the glenohumeral joint in MS, requiring a compensation of humeral axial rotation to bring the hand markers closer to their experimental locations. Even if WAD evolution of thorax and pelvis was zero on average, spine degrees of freedom were influenced by the model choice. Besides, more GL and inconsistent results were reported with MS, conducting to non-physiological values for joint kinematics. However, only one kinematic sequence was taken into account whereas some authors (Senk and Cheze 2006) proved its choice may have an influence on GL.

Finally, this study demonstrated the decisive effect of the shoulder model to efficiently track the upper-body kinematics during the golf swing based on MKO technique. The advantage of MKO is to provide consistent joint kinematics (avoiding joint dislocations and bones penetrations in reconstructed kinematics) and to limit the effect of STA. However, its efficiency fully relies on the model definition. These models include joint definitions with DoF but also locations of these joints. In the present study, the effect of DoF was investigated but results would also be affected by the location of the joint. Hence particular attention would also be paid to the adaptation of the model to individuals. This personalization procedure is considered by some authors as one of the main challenges for the years to come (Duprey et al., 2016), and in particular the clavicle length (i.e. distance between SCJ and ACJ) which has already been proved to be decisive (El Habachi et al., 2015).

Conflict of interest

The authors declare they have no financial or personal relationships with other people or organization that could inappropriately influence their work.

References

- Andersen M.S., Benoit D.L., Damsgaard M, Ramsey D.K., Rasmussen J., 2010. Do kinematic models reduce the effects of soft tissue artefacts in skin marker-based motion analysis? An in vivo study of knee kinematics. *Journal of Biomechanics*, 43(2), 268-273.
- Blache, Y., Dumas, R., Lundberg, A., Begon, M., 2016. Main component of soft tissue artifact of the upper-limbs with respect to different functional, daily life and sports movements. *Journal of Biomechanics*
- Bourgain, M., Sauret, C., Rouch, P., Thoreux, P., Rouillon, O., 2016. Evaluation of the Spine Axial Rotation Capacity of Golfers and its Distribution. *Human Kinetics.*
- Cole, M.H., Grimshaw, P.N., 2014. The crunch factor's role in golf-related low back pain. *Spine Journal* 14, 799–807.
- Dal Maso, F., Raison, M., Lundberg, A., Arndt, A., Begon, M., 2014. Coupling between 3D displacements and rotations at the glenohumeral joint during dynamic tasks in healthy participants. *Clinical Biomechanics* Bristol Avon 29, 1048–1055.
- Delp, S.L., Anderson, F.C., Arnold, A.S., Loan, P., Habib, A., John, C.T., Guendelman, E., Thelen, D.G., 2007. OpenSim: open-source software to create and analyze dynamic simulations of movement. *IEEE Transactions Biomedical* Eng. 54, 1940–1950.
- Delp, S.L., Loan, J.P., Hoy, M.G., Zajac, F.E., Topp, E.L., Rosen, J.M., 1990. An interactive graphics-based model of the lower extremity to study orthopaedic surgical procedures. *IEEE Transactions Biomedical* Eng. 37, 757–767.
- Duprey, S., Naaim, A., Moissenet, F., Begon, M., Chèze, L., 2016. Kinematic models of the upper limb joints for multibody kinematics optimisation: An overview. *Journal of Biomechanics.* 0.
- Egret, C., Dujardin, F., Weber, J., Chollet, D., 2004. 3D Kinematic analysis of the golf swings of expert and experienced golfers. *Journal of Human movement studies.*
- Egret, C.I., Vincent, O., Weber, J., Dujardin, F.H., Chollet, D., 2003. Analysis of 3D kinematics concerning three different clubs in golf swing. *International Journal of Sports Medicine* 24, 465–470.
- Gluck, G.S., Bendo, J.A., Spivak, J.M., 2008. The lumbar spine and low back pain in golf: a literature review of swing biomechanics and injury prevention. *Spine Journal: Official Journal of the North American Spine Society* 8, 778–788.
- Habachi, A.E., Duprey, S., Cheze, L., Dumas, R., 2015. A parallel mechanism of the shoulder—application to multi-body optimisation. *Multibody System Dynamics.* 33, 439–451.
- Joyce, C., Burnett, A., Ball, K., 2010. Methodological considerations for the 3D measurement of the X-factor and lower trunk movement in golf. *Sports Biomechanics.* 9, 206–221.
- Healy, A., K.A. Moran, J. Dickson, C. Hurley, A.F. Smeaton, N.E. O'Connor, P. Kelly, M. Haahr, and N. Chockalingam. 2011. Analysis of the 5 Iron Golf Swing When Hitting for Maximum Distance. *Journal of Sports Sciences* 29 (10): 1079–88
- Kwon, Y.-H., Han, K.H., Como, C., Lee, S., Singhal, K., 2013. Validity of the X-factor computation methods and relationship between the X-factor parameters and clubhead velocity in skilled golfers. *Sports Biomechanics.* 12, 231–246.
- Lu, T.W., O'Connor, J.J., 1999. Bone position estimation from skin marker co-ordinates using global optimisation with joint constraints. *Journal of Biomechanics.* 32, 129–134.
- Matsui, K., Shimada, K., Andrew, P.D., 2006. Deviation of skin marker from bone target during movement of the scapula. *Journal of Orthopedic Sciences.* 11, 180–184.
- McClure, P.W., Michener L.A., Sennett B.J., Karduna A.R., 2001. Direct 3-dimensional measurement of scapular kinematics during dynamic movements in vivo. *Journal of Shoulder and Elbow Surgery.* 10, 269-277.

- McHardy, A., Pollard, H., 2005. Lower back pain in golfers: a review of the literature. *Journal of Chiropractic Medicine*. 4, 135–143.
- McHardy, A., Pollard, H., Luo, K., 2006. Golf injuries: a review of the literature. *Sports Medicine Auckland*. NZ 36, 171–187.
- Myers, J., Lephart, S., Tsai, Y.-S., Sell, T., Smoliga, J., Jolly, J., 2008. The role of upper torso and pelvis rotation in driving performance during the golf swing. *Journal of Sports Sciences*. 26, 181–188.
- Naaim, A., Moissenet, F., Dumas, R., Begon, M., Chèze, L., 2015. Comparison and validation of five scapulothoracic models for correcting soft tissue artefact through multibody optimisation. *Computational Methods in Biomechanics and Biomedical* Engineering. 18 Suppl 1, 2014–2015.
- Naaim, A., Moissenet, F., Duprey, S., Begon, M., Chèze, L., 2017. Effect of various upper limb multibody models on soft tissue artefact correction: A case study. *Journal of Biomechanics*. 0.
- Nesbit, S.M., 2005. A Three Dimensional Kinematic and Kinetic Study of the Golf Swing. *Journal of Sports Sciences in Medicine* 4, 499–519.
- Perron, C., Rouillon, O., Edouard, P., 2016. Epidemiological study on injuries and risk factors for injuries in the amateur golfer French high-level. *Annals of Physical and Rehabilitation Medicine*, 31st Annual Congress of the French Society of Physical and Rehabilitation Medicine 59, Supplement, e20.
- Prinold, J.A.I., Bull, A.M.J., 2014. Scaling and kinematics optimisation of the scapula and thorax in upper limb musculoskeletal models. *Journal of Biomechanics* 47, 2813–2819.
- Raabe, M.E., Chaudhari, A.M.W., 2016. An investigation of jogging biomechanics using the full-body lumbar spine model: Model development and validation. *Journal of Biomechanics*. 49, 1238–1243.
- Senk, Miroslav, and Laurence Chèze. 2006. Rotation Sequence as an Important Factor in Shoulder Kinematics. *Clinical Biomechanics* (Bristol, Avon) 21 Suppl 1: S3–8.
- Seth, A., Matias, R., Veloso, A.P., Delp, S.L., 2016. A Biomechanical Model of the Scapulothoracic Joint to Accurately Capture Scapular Kinematics during Shoulder Movements. *PLoS ONE* 11, e0141028.

Supplementary material

Table SM1: Definition of the markers used in this study. The third column is the weight used for the different markers for the model positioning during the scaling procedure in the static pose. The fourth column is the weight used for performing the inverse kinematics processing during the golf swing. The last column defined to which segment a marker and its kinematic weight was associated for calculation of the segment weighted average distance (WAD).

Anatomical landmark	Defined in	Weight scaling	Weight kinematics	Associated segment for WAD computation
Manubrium	Thorax	10	10	Thorax, Clavicle
Xyphoid process	Thorax	5	10	Thorax
7th cervicale vertebra	Thorax	10	10	Thorax
8th thoracic vertebra	Thorax	2	10	Thorax
12th thoracic vertebra	Thorax	2	10	Thorax
5th lumbar vertebra	Thorax	0	10	
Thorax technical markers (2 markers)	Thorax	0 (x2)	5 (x2)	Thorax
Middle of the clavicle	Clavicle	0	10	Shoulder, Clavicle
Acromion	Scapula	10	10	Shoulder, Scapula, Clavicle
Scapula spine marker cluster (3 markers)	Scapula	0 (x3)	6 (x3)	Shoulder, Scapula
Lateral epicondyle	Humerus	10	10	Arm
Radial styloïd process	Radius	10	10	Arm
Radius technical marker	Radius	0	5	Arm
Ulnar styloïd process	Ulna	10	10	Arm
2nd metacarpus	Hand	10	10	Hand
5th metacarpus	Hand	0	10	Hand
Antero-superior iliac spine	Pelvis	10	10	Pelvis
Postero-superior iliac spine	Pelvis	10	10	Pelvis
Pelvis technical marker	Pelvis	0	5	Pelvis

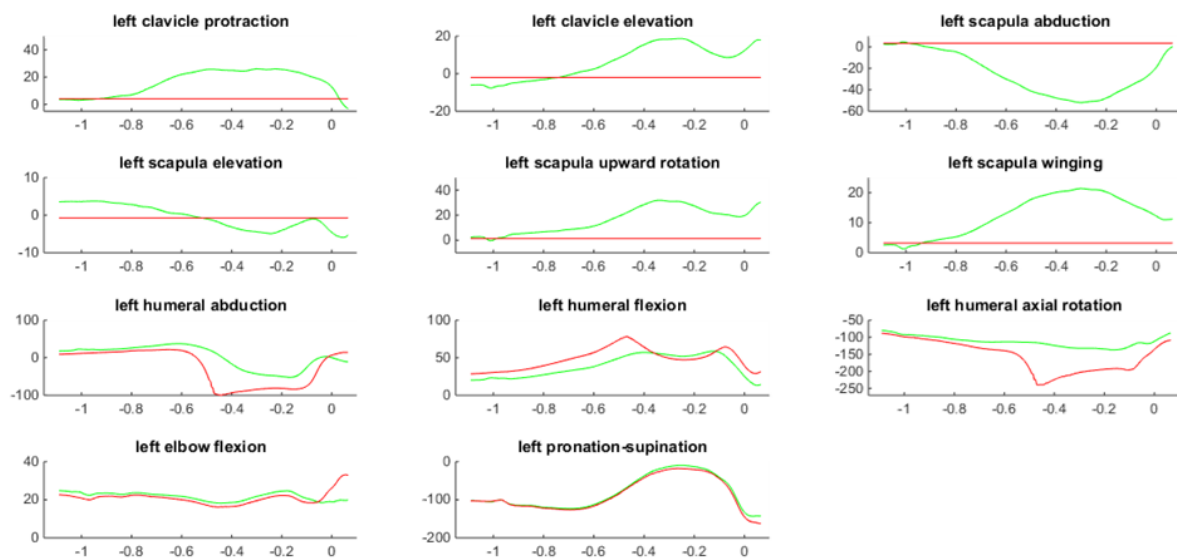|				
Femur marker cluster (4 markers)	Femur	0 (x4)	5 (x4)	Thigh
Femur medial condyle	Femur	10	10	Thigh , Leg
Femur lateral condyle	Femur	10	10	Thigh , Leg
Fibula head	Fibula	0	10	Leg
Technical marker of the tibia	Tibia	0	10	Leg
Medial malleolus	Tibia	10	10	Leg
Lateral malleolus	Fibula	10	10	Leg
Calcaneum	Foot	0	10	Foot
Technical marker of the calcaneum	Foot	0	10	Foot
1st metatarsus	Foot	10	10	Foot
5th metatarsus	Foot	0	10	Foot
Technical marker of the foot	Foot	0	5	Foot

Figure SM1 : Differences in left shoulder and elbow kinematics during a swing (best swing of subject 1) computed with MS (red) and MP (green) models.
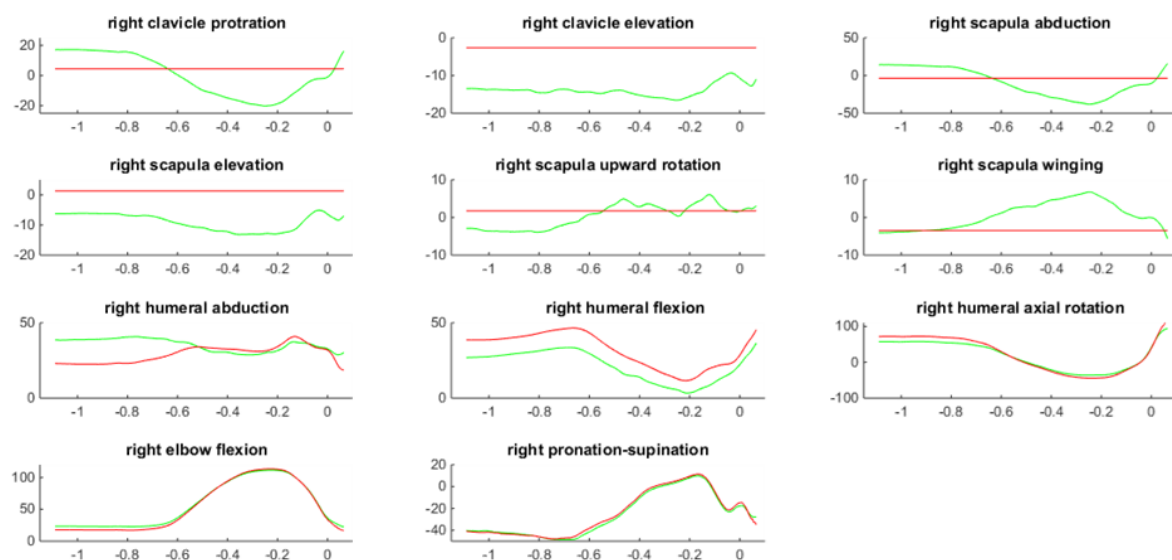

Figure SM2 : Differences in right shoulder and elbow kinematics during a swing (best swing of subject 1) computed with MS (red) and MP (green) models.
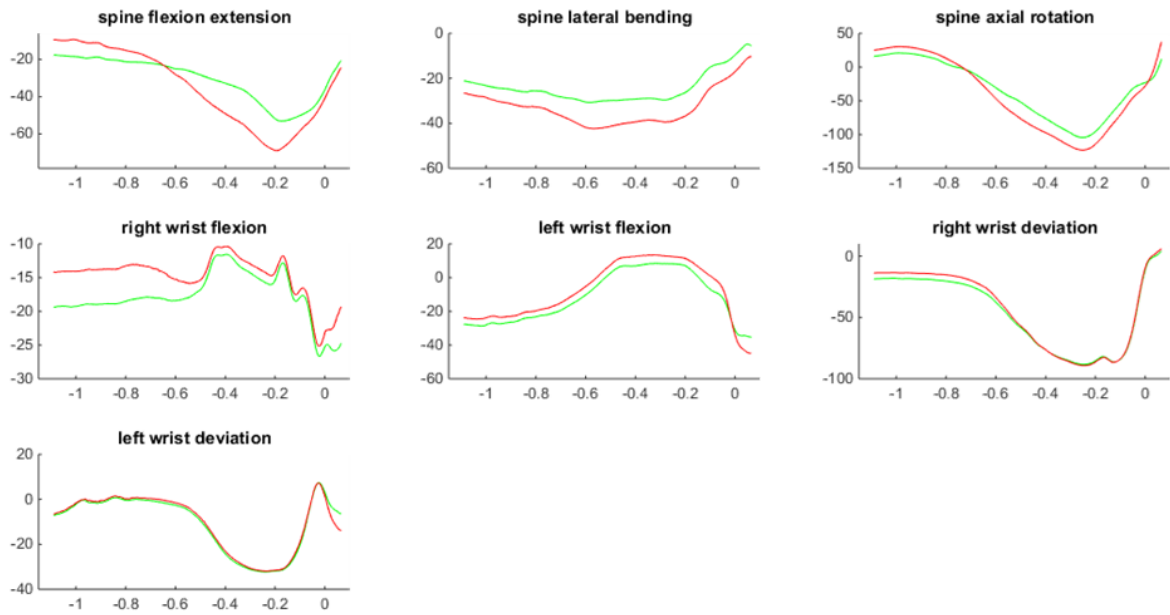
Figure SM3 : Differences in spine and wrists kinematics during a swing (best swing of subject 1) computed with MS (red) and MP (green) models.